

Frequency Domain Analysis of Lifting Problems with Explicit Kutta Condition

Jong-Un Kim¹, Gun-Do Kim¹ and Chang-Sup Lee¹

¹Chungnam National University; E-mail: csleepro@cnu.ac.kr

Abstract

Explicit Kutta condition approximation, proved useful in existing time-domain solver of the unsteady propeller problem, requires a specified functional behavior of the vorticity in space near the trailing edge. In this paper, the strength of the discrete vortices is controlled to have a specified behavior in space in the frequency domain approach. A new formulation is introduced and is implemented for analysis of a lifting surface of a rectangular planform. Sample computations carried out according to the new formulation compares well with that of existing unsteady lifting problem in the time domain.

Keywords: lifting surface, discrete vortex method, frequency domain approach, explicit Kutta condition

1 Introduction

In recent decades, for the theoretical prediction of propeller performances, the unsteady lifting surface theory has been widely used by most of the propeller designers around the world. This theory, formulated under the assumption of the potential flow, is proved to be practically accurate enough for the design and analysis of the propeller operating in the vortical flow generated by the ship. The vortex lattice method (VLM) of Kerwin(1961) is one of the pioneering works successfully applied to the solution of the propeller lifting surface problems and extended to the design of the propeller blades(Kerwin 1973). This method was modified and applied by Cummings(1973) for the analysis of the steady performance of the propellers and by Tsao(1975) for the analysis of controllable-pitch propellers, adopting the mode function approach to represent the radial and chordwise variation of the vortices. The mode function method suffered the convergence problem as the number of modes increased. Kerwin and Lee(1978) then suggested a new VLM, where concentrated vortices were placed on the camber surface of the propeller blades, and could compute the unsteady performance of propellers operating in nonuniform ship flows.

There exist various lifting surface theories, including the continuous vortex method (CVM), continuous dipole method (CDM) and discrete vortex method (DVM). The CVM, as demonstrated by Chow(1979), suffered a convergence problem due to the omission of the control points near the leading edge. The CDM according to Moran(1984) is found superior to Chow. The DVM, suggested originally by Falkner, is successfully applied for the solution of the lifting problems of the airplane wing and propeller blades. In DVM, the continuous distribution of the vortices is replaced by a lattice of concentrated vortices and the boundary conditions are satisfied on a set

of selected control points to determine the strength of the discrete vortices. For a 2-dimensional wing, James(1972) showed that by dividing the chord length into a uniformly spaced segments and by placing the discrete vortices and control points on the 1/4 and 3/4 chord of each segment, respectively, the Kutta condition at the trailing edge is automatically satisfied.

For the unsteady lifting problem, both the time and frequency domain analysis methods can be used. Since Kerwin and Lee(1978) adopted the time domain approach, Lee(1977) and Lee(1979) followed this line, because the propeller cavity problem could be solved only in the time domain as shown in Lee(1979). The cavity extent on the propeller blade surface, which is essential in placing the cavity sources, could not be represented by a Fourier series. The strength of the cavity sources and vortices, which is a function of the time and space, could not be represented by the Fourier series. The frequency domain approach however has a merit in case when all the loadings can be represented by Fourier series and when the amplitude of Fourier series terms dies out rapidly as the order of the series increases. One of the successful applications of the frequency domain approach for DVM may be Kim and Lee(1981), who solved the unsteady hydrofoil problem extending to the analysis of the fish propulsion. Chai(1990) solved the same two-dimensional problem both in the time and frequency domains. Chai satisfied the Kutta condition by specifying the time step such that the spacing of the discrete vortices on the foil and in the wake be identical.

There are cases where the frequency domain solution is needed. One is the theoretical evaluation of the relative rotative efficiency η_R . The propeller operating in non-uniform ship wake requires less torque than the propeller in open water at the same thrust loading, leading to $\eta_R > 1.0$. This is considered caused by the mean leading edge suction force arising from the high order frequency components. The disadvantage of the time domain approach can be the relative large CPU time. Although this can not be the drawback when the unsteady propeller problem is solved only few times, this may become serious if many calls to this unsteady propeller solver are needed. One example may be the skew optimization problem, where the unsteady propeller solver is called in an infinite optimization loop until a desired accuracy is reached. If we agree that first few terms of the forces represented in Fourier series are mostly significant, we may reduce the CPU drastically in estimating the global unsteady propeller force level. This is likely to be sufficient for skew optimization problem.

There is however a reason why the propeller unsteady problem, even for the non-cavitating case, is not yet solved using DVM in frequency domain. The accuracy of Kerwin and Lee(1978), satisfying all the users, has to be maintained under any circumstances. The DVM of Kerwin and Lee adopted the explicit Kutta condition which strongly control the behavior of the vortex strengths at or near the trailing edge of the blade. The control in the space could easily be implemented in the time domain approach as is evidenced in Kerwin and Lee, but could not be achieved in frequency domain approach so far. The main purpose of this paper is to formulate the vortex lattice method with the explicit Kutta condition in frequency domain. The formulation will then be applied for the solution of the unsteady 3-dimensional wing problem.

2 Integral equation

Let us consider a 3-dimensional hydrofoil advancing at a uniform speed U in an ideal fluid represented by (1) as:

$$h = h(x, z; t) \tag{1}$$

We define a body-fixed coordinate system with x-axis positive downstream, the y-axis upward, the z-axis pointing port side of the hydrofoil as shown in Figure 1.

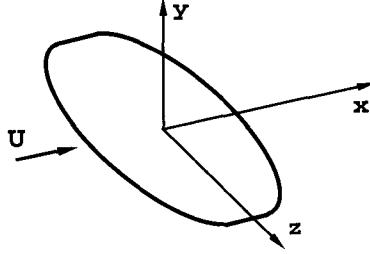


Figure 1: Three-dimensional hydrofoil and the body-fixed coordinate system

We will replace the hydrofoil and the trailing wake with the vorticity $\vec{\gamma}(\vec{\xi}, t)$ in the horizontal $x - z$ plane, then the induced velocity integral may be expressed as:

$$v(\vec{x}, t) = \iint_{Foil+Wake} \gamma(\vec{\xi}, t) K(\vec{x}, \vec{\xi}) d\sigma \quad (2)$$

where $K(\vec{x}, \vec{\xi})$ is the induced velocity at \vec{x} due to unit strength vorticity in the hydrofoil or wake surface at $\vec{\xi}$.

Applying the kinematic boundary condition $DF/Dt = 0$, where $F = y - h = 0$ is the surface function, on the foil surface, we obtain:

$$v = \frac{\partial h}{\partial t} + U \frac{\partial h}{\partial x} \quad (3)$$

From Equations (2) and (3) we obtain the following:

$$\iint_{Foil} \gamma(\vec{\xi}, t) K(\vec{x}, \vec{\xi}) d\sigma = - \iint_{Wake} \gamma(\vec{\xi}, t) K(x, \vec{\xi}) d\sigma + \frac{\partial h}{\partial t} + U \frac{\partial h}{\partial x} \quad (4)$$

Because the vorticity in the wake can be expressed as a function of the vorticity on the foil in the past by applying Kelvin's theorem and the dynamic boundary condition in the wake, Equation (4) becomes an integral equation for the determination of the vorticity on the foil. Once the integral equation is solved, the lift on the foil can be obtained by integrating the pressures on both sides of the hydrofoil as follows:

$$\begin{aligned} L &= - \iint_{Foil} (P - P_\infty) d\sigma \\ &= \rho \iint_{Foil} \frac{\partial \phi}{\partial t} d\sigma - \frac{\rho U}{2} \iint_{Foil} \gamma_b d\sigma \end{aligned} \quad (5)$$

where P and P_∞ are the pressure on the foil surface and the reference pressure at the infinity upstream, respectively, ρ the density of the fluid, and γ_b is the bound vorticity normal to the free stream velocity vector. The first term in the right-hand side of Equation (5) is the added mass term, and the second term is the quasi-steady term.

3 Discretization of vorticity

For the numerical computation of (4), the continuous distribution of the vorticity $\vec{\gamma}(\vec{x}, t)$ is replaced by a lattice of discrete vortex segments, as shown in Figure 2 typically for a hydrofoil of the rectangular planform. The vortex lattice consists of N bound(spanwise) vortex elements Γ^s along

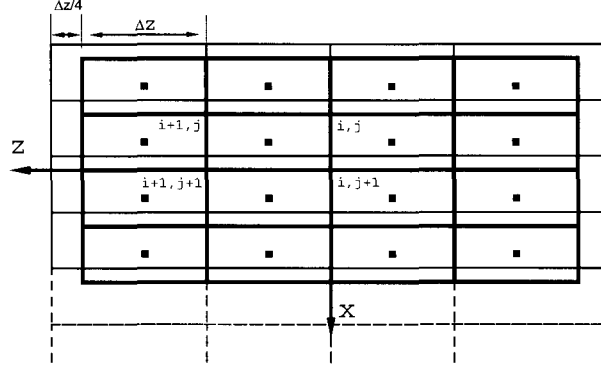


Figure 2: Discrete vortex lattice representation of a hydrofoil of rectangular plan form

each chordwise strip and $M + 1$ free(chordwise) vortex elements Γ^c extending from the leading edge to infinity downstream. The vortex lattice thus forms $N \times M$ closed vortex loops. The last spanwise vortex together with the free vortex extending to infinity downstream will form a horseshoe vortex for the steady problem, but in the unsteady problem there exists shed vortex segments which are in the $x - z$ plane and loosely in the direction normal to the free stream. We will use the terms spanwise and chordwise instead of the terms bound and free. For a three-dimensional hydrofoil of arbitrary plan form in the general 3-dimensional flow, the chordwise vortex segment is no longer force-free, and the spanwise vortex elements are not the only vortex “bound” to the foil to sustain the forces acting on the hydrofoil. The discrete vortex arrangement and the terminology follow the convention of Kerwin and Lee(1978).

For a two-dimensional flat plate wing, James(1972) shows that the 1/4-3/4 arrangement of the vortices and control points produces the loading to a remarkable accuracy. James subdivided the chord c into N elements of equal chord-segment $\Delta x = c/N$, and located the discrete vortex on the 1/4 chord of each segment and the control point on the 3/4 chord of each segment. The x -coordinate of the j -th spanwise vortex is then expressed as:

$$x_j^v = -\frac{c}{2} + (j + \frac{1}{4})\frac{c}{N}, \quad (j = 0, 1, 2, \dots, N - 1) \quad (6)$$

In the spanwise direction, the span is divided into M panels of equal length Δz with the tip coordinate inserted by $\Delta z/4$ at both tips. The z -coordinate of the i -th chordwise vortex of this spanwise uniform discretization is then expressed as:

$$z_i^v = -\frac{s}{2} + \Delta z(i + \frac{1}{4}), \quad (i = 0, 1, 2, \dots, M) \quad (7)$$

where $\Delta z = s/(M + 0.5)$ and s the span of the foil. At the (i, j) -th intersection, the vectoral form of the intersection may be written as $\vec{x}_{i,j}^v = (x_j^v, 0, z_i^v)$.

The control points, where the impermeability condition is satisfied, are located at the geometric center of each quadrilateral lattice loop and are expressed for the (i, j) -th control point as:

$$\bar{x}_{i,j}^p = \frac{1}{4}(\bar{x}_{i,j}^v + \bar{x}_{i,j+1}^v + \bar{x}_{i+1,j}^v + \bar{x}_{i+1,j+1}^v) \quad (8)$$

4 Kutta condition

The Kutta condition requires that the flow departs from the trailing edge in a smooth manner and that the pressure jump between the upper and lower surfaces at the trailing edge vanishes. For a two-dimensional flat plate, James showed that the 1/4-3/4 arrangement leads to the correct behavior of the loading distribution at the trailing edge as the number of discrete vortices increases. In the unsteady problem of the hydrofoil, the smoothness of the flow across the trailing edge can be obtained by determining the advance distance per time step Δw be identical to panel size on the foil Δc , that is $\Delta w = \Delta c$. Because the behavior of the vortex strength is controlled by discretization only, this is called the implicit numerical Kutta condition. Contrary to this, the explicit numerical Kutta condition specifies the behavior of the vorticity variation in the neighborhood of the trailing edge by a function. The advantage is that by specifying the behavior of the vorticity the control points may be removed near or close to the trailing edge. This feature is needed when the condition of $\Delta w = \Delta c$ can not be met in the spanwise direction on the hydrofoil of elliptic planform or in the radial direction on the propeller.

A numerical form of an explicit Kutta condition is due to Kerwin and Frydelund(1977), where they specified the quadratic variation of the vorticity on the blade near the trailing edge and the linear variation of the shed vorticity on the wake just downstream of the trailing edge. Another form is due to Kerwin and Lee(1978), where they specify the linear variation of the vorticity on the blade and no specific variation in the wake except that the vorticity on the blade and in the wake be continuous at the trailing edge.

We follow the approach of Kerwin and Lee, which is already validated in the unsteady propeller analysis. Assuming that the vorticity varies linearly adjacent to the trailing edge as shown in Figure 3, the strength of the discrete vortex on the blade, Γ_{N-2}^s and Γ_{N-1}^s , and the strength of the first shed vortex Γ_0^{ws} can be expressed as:

$$\begin{aligned} \Gamma_{N-2}^s &= C_0 \sum_{j=0}^{N-4} \Gamma_j^s + C_1 \Gamma_{N-3}^s + C_2 \sum_{k=1}^{N^w-1} \Gamma_k^{ws} \\ \Gamma_{N-1}^s &= C_3 \sum_{j=0}^{N-4} \Gamma_j^s + C_4 \Gamma_{N-3}^s + C_5 \sum_{k=1}^{N^w-1} \Gamma_k^{ws} \\ \Gamma_0^{ws} &= C_6 \sum_{j=0}^{N-4} \Gamma_j^s + C_7 \Gamma_{N-3}^s + C_8 \sum_{k=1}^{N^w-1} \Gamma_k^{ws} \end{aligned} \quad (9)$$

where

$$\begin{aligned}
 C_0 &= \frac{-e'}{1+e'+g'}, & C_1 &= \frac{d(1+g')-e'(1+f)}{1+e'+g'}, & C_2 &= C_0 \\
 C_3 &= \frac{-g'}{1+e'+g'}, & C_4 &= \frac{f(1+e')-g'(1+d)}{1+e'+g'}, & C_5 &= C_3 \\
 C_6 &= \frac{-1}{1+e'+g'}, & C_7 &= \frac{-f(1+d+f)}{1+e'+g'}, & C_8 &= C_6 \\
 e' &= e\left(\frac{\Delta f}{\Delta w}\right), & g' &= g\left(\frac{\Delta f}{\Delta w}\right)
 \end{aligned}$$

The symbols a, d, e , etc are defined in Appendix A, together with the derivation leading to (9).

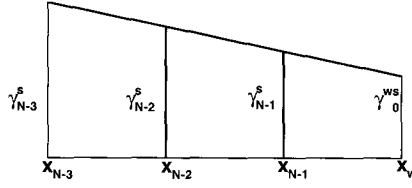


Figure 3: Spanwise vorticity variation for two-point linear Kutta condition

5 Analysis in frequency domain

For a steadily oscillating motion, the strength of the j -th discrete vortex $\Gamma_j(t)$ responding to the external forces of angular frequency ω may be expressed simply as:

$$\Gamma_j(t) = \Gamma_c^j \cos \omega t + \Gamma_s^j \sin \omega t \quad (10)$$

The total circulation on the hydrofoil at a give time t may now be expressed as:

$$\begin{aligned}
 \Gamma^T(t) &= \sum_{j=0}^{N-1} [\Gamma_c^j \cos \omega t + \Gamma_s^j \sin \omega t] \\
 &= \left[\sum_{j=0}^{N-1} \Gamma_c^j \right] \cos \omega t + \left[\sum_{j=0}^{N-1} \Gamma_s^j \right] \sin \omega t
 \end{aligned} \quad (11)$$

Applying Kelvin's theorem of circulation conservation and the dynamic boundary condition in the wake(Newman 1977), we obtain the expression for the vorticity at the trailing edge $\gamma(c, t)$ as a derivative of the total circulation as:

$$\frac{d\Gamma^T}{dt} = -U\gamma(c, t) \quad (12)$$

From Equations (11) and (12), the vorticity at the trailing edge may be expressed in terms of cosine and sine amplitudes of the discrete vortex strengths as:

$$\gamma(c, t) = -\frac{\omega}{U} \left\{ \left[-\sum_{j=0}^{N-1} \Gamma_c^j \right] \sin \omega t + \left[\sum_{j=0}^{N-1} \Gamma_s^j \right] \cos \omega t \right\} \quad (13)$$

Analysis in the frequency domain does not require the time step for the time derivative, but the wake spacing $\Delta w = U\Delta t$ is necessary to compute the history of shed vortices in discrete space. Although the wake spacing defined in this way is not essential in the frequency domain analysis, it is taken here this way for simplicity. The first discrete vortex strength in the wake Γ_0^{ws} may now be expressed as:

$$\begin{aligned}\Gamma_0^{ws} &= -\gamma(c, t)U\Delta t \\ &= -\omega\Delta t[-\sum_{j=0}^{N-1} \Gamma_c^j] \sin \omega t + [\sum_{j=0}^{N-1} \Gamma_s^j] \cos \omega t\end{aligned}\quad (14)$$

Conservation of the circulation on a node $\vec{x}_{i,j}$ where the chordwise vortex segment start gives the relation between the chordwise and spanwise vortex segments, $\Gamma_{i,j}^c$ and $\Gamma_{i,j}^s$, respectively, as:

$$\begin{aligned}\Gamma_{i,j}^c &= \Gamma_{i-1,j}^s + \Gamma_{i,j-1}^c - \Gamma_{i,j}^s \\ &= \sum_{l=0}^j \Gamma_{i-1,l}^s - \sum_{l=0}^j \Gamma_{i,l}^s, \quad (i = 0, 1, 2, \dots, M)\end{aligned}\quad (15)$$

The strength of the first shed vortex can also be obtained by applying Kelvin's theorem on a chordwise strip on the hydrofoil and its trailing wake extending to downstream infinity, that is:

$$\Gamma_{i,0}^{ws} = -[\sum_{j=0}^{N-1} \Gamma_{i,j}^s + \sum_{k=1}^{N^w-1} \Gamma_{i,k}^{ws}]\quad (16)$$

where N^w is the number of shed vortices in the wake.

Upon discretization of the continuous vortex sheet into a lattice of discrete vortices, the surface integrals in Equation (4) can be transformed into double summation of induced velocities due to discrete vortices and hence Equation (4) becomes:

$$\begin{aligned}&\sum_{i=0}^{M-1} \sum_{j=0}^{N-1} \Gamma_{i,j}^s v(\vec{x}_p; \vec{x}^s) + \sum_{i=0}^M \sum_{j=0}^{N-1} \Gamma_{i,j}^c v(\vec{x}_p; \vec{x}^c) \\ &= -\sum_{i=0}^{M-1} \Gamma_{i,0}^{ws} v(\vec{x}_p; \vec{x}^w) - \sum_{i=0}^{M-1} \sum_{k=1}^{N^w-1} \Gamma_{i,k}^{ws} v(\vec{x}_p; \vec{x}^{ws}) \\ &\quad - \sum_{i=0}^M \sum_{k=0}^{N^w-2} \Gamma_{i,k}^{wc} v(\vec{x}_p; \vec{x}^{wc}) + \frac{\partial h}{\partial t} + U \frac{\partial h}{\partial x}\end{aligned}\quad (17)$$

where the induced velocity at a control point due to a unit strength vortex segment $\vec{v}(\vec{x}_p; \vec{x})$ is computed by Biot-Savart's law:

$$\vec{v}(\vec{x}_p; \vec{x}) = \frac{1}{4\pi} \int_{\delta\ell} \frac{d\vec{\ell} \times \vec{D}}{D^3}\quad (18)$$

The first and second summations in the left-hand side of Equation (17) are induced velocities due to a set of spanwise vortex segments Γ^s and chordwise vortex segments Γ^c . The first summation

in the right-hand side is the induced velocity due to the first shed vortices in the wake, and the second and third summations are those due to shed vortices and streamwise vortices.

Substituting Equations (15), (16) and numerical Kutta condition (9) into Equation (17) will result, after some manipulation:

$$\begin{aligned}
 & \sum_{i=0}^{M-1} \left\{ \sum_{j=0}^{N-4} [F(\vec{x}_p; i, j) + C_0 F(\vec{x}_p; i, N-2) + C_3 F(\vec{x}_p; i, N-1)] \Gamma_{i,j}^s \right. \\
 & \quad \left. + F[(\vec{x}_p; i, N-3) + C_1 F(\vec{x}_p; i, N-2) + C_4 F(\vec{x}_p; i, N-1)] \Gamma_{i,N-3}^s \right\} \\
 = & \sum_{i=0}^{M-1} [v(\vec{x}_p; \vec{x}^w) - C_2 F(\vec{x}_p; i, N-2) - C_5 F(\vec{x}_p; i, N-1)] \left[\sum_{k=1}^{N^w-1} \Gamma_{i,k}^{ws} \right] \\
 & - \sum_{i=0}^{M-1} \sum_{k=1}^{N^w-1} v(\vec{x}_p; \vec{x}^{ws}) \Gamma_{i,k}^{ws} - \sum_{i=0}^M \sum_{k=0}^{N^w-2} v(\vec{x}_p; \vec{x}^{wc}) \Gamma_{i,k}^{wc} \\
 & + \frac{\partial h}{\partial t} + U \frac{\partial h}{\partial x}
 \end{aligned} \tag{19}$$

where

$$F(\vec{x}_p; i, j) \equiv v(\vec{x}_p; \vec{x}^s) - v(\vec{x}_p; \vec{x}^w) + \sum_{l=j}^{N-1} [v(\vec{x}_p; \vec{x}_{i+1,l}^c) - v(\vec{x}_p; \vec{x}_{i,l}^c)]$$

The vortex in the wake in Equation (18) may be converted into closed vortex loops, as derived in Appendix B, as follows:

$$\begin{aligned}
 & \sum_{i=0}^{M-1} \left\{ \sum_{j=0}^{N-4} [F(\vec{x}_p; i, j) + C_0 F(\vec{x}_p; N-2) + C_3 F(\vec{x}_p; N-1)] \Gamma_{i,j}^s \right. \\
 & \quad \left. + [F(\vec{x}_p; i, N-3) + C_1 F(\vec{x}_p; N-2) + C_4 F(\vec{x}_p; N-1)] \Gamma_{i,N-3}^s \right\} \\
 = & \sum_{i=0}^{M-1} \{ [-C_2 F(\vec{x}_p; i, N-2) - C_5 F(\vec{x}_p; i, N-1)] \\
 & \quad \times \sum_{k=1}^{N^w-1} [-\Gamma_i^T(t = \tau - k) + \Gamma_i^T(t = \tau - k - 1)] \} \\
 & + \sum_{i=0}^{M-1} \sum_{k=1}^{N^w-1} v_{i,k}^{w\Box} [-\Gamma_i^T(t = \tau - k)] \\
 & + \frac{\partial h}{\partial t} + U \frac{\partial h}{\partial x}
 \end{aligned} \tag{20}$$

where Γ_i^T is the total circulation on the i -th chordwise strip, and the superscript \Box denotes the quadrilateral loop vortices.

Substituting Equation (14) into the numerical Kutta condition relation (35), we obtain:

$$\begin{aligned}\Gamma_{N-2}^s &= d\Gamma_{N-3}^s + e\left(\frac{\Delta f}{\Delta\omega}\right)\left\{\omega\Delta t\left[\left(\sum_{j=0}^{N-1}\Gamma_{jc}^s\right)\sin\omega t - \left(\sum_{j=0}^{N-1}\Gamma_{js}^s\right)\cos\omega t\right]\right\} \\ \Gamma_{N-1}^s &= f\Gamma_{N-3}^s + g\left(\frac{\Delta f}{\Delta\omega}\right)\left\{\omega\Delta t\left[\left(\sum_{j=0}^{N-1}\Gamma_{jc}^s\right)\sin\omega t - \left(\sum_{j=0}^{N-1}\Gamma_{js}^s\right)\cos\omega t\right]\right\}\end{aligned}\quad (21)$$

The total circulation Γ_i^T may be rewritten, omitting the subscript index i as:

$$\begin{aligned}\Gamma^T(t) &= \sum_{j=0}^{N-4}\Gamma_j^s + \Gamma_{N-3}^s + \Gamma_{N-2}^s + \Gamma_{N-1}^s \\ &= \left[\sum_{j=0}^{N-4}\Gamma_{jc}^s + (\Gamma_{N-3})_c + (\Gamma_{N-2})_c + (\Gamma_{N-1})_c\right]\cos\omega t \\ &\quad + \left[\sum_{j=0}^{N-4}\Gamma_{js}^s + (\Gamma_{N-3})_s + (\Gamma_{N-2})_s + (\Gamma_{N-1})_s\right]\sin\omega t\end{aligned}\quad (22)$$

After substituting Equation (21) into (22), we may derive expressions for $\Gamma_i^T(t = \tau - k)$ $\Gamma_i^T(t = \tau - k - 1)$. These can then be inserted into Equation (20) with $\Gamma_j^s(\tau)$ replaced by (10). Requiring the coefficients of $\cos\omega\tau$ and $\sin\omega\tau$ to vanish, we may arrive at the following(see Appendix C for details):

$$\begin{bmatrix} I & II \\ III & IV \end{bmatrix} \begin{bmatrix} (\Gamma_{i,j}^s)_c \\ (\Gamma_{i,j}^s)_s \end{bmatrix} = RHS \quad (23)$$

where the submatrices I, II, III and IV are all $[(N-2) \times M] \times [(N-2) \times M]$ square matrices,

and have the elements of the following form:

$$\begin{aligned}
 I_{i,j} &= \sum_{i=0}^{M-1} \left[\sum_{j=0}^{N-4} [(F_{i,j}^*)_1 + \sum_{k=1}^{N^w-1} [(C_{00}^{**})_k((F_i^*)_2 + v_{i,k}^{w\Box}) - (C_{20}^{**})_k(F_i^*)_2]](\Gamma_{i,j}^s)_c \right. \\
 &\quad \left. + [(F_{i,N-3}^*)_1 + \sum_{k=1}^{N^w-1} [(C_{10}^{**})_k((F_i^*)_2 + v_{i,k}^{w\Box}) - (C_{30}^{**})_k(F_i^*)_2]](\Gamma_{i,N-3}^s)_c \right. \\
 II_{i,j} &= \sum_{j=0}^{N-4} \left[\sum_{k=1}^{N^w-1} [(C_{01}^{**})_k((F_i^*)_2 + v_{i,k}^{w\Box}) - (C_{21}^{**})_k(F_i^*)_2]](\Gamma_{i,j}^s)_s \right. \\
 &\quad \left. + \left[\sum_{k=1}^{N^w-1} [(C_{11}^{**})_k((F_i^*)_2 + v_{i,k}^{w\Box}) - (C_{31}^{**})_k(F_i^*)_2]](\Gamma_{i,N-3}^s)_s \right] \right. \\
 III_{i,j} &= \sum_{i=0}^{M-1} \left[\sum_{j=0}^{N-4} \left[\sum_{k=1}^{N^w-1} [(C_{02}^{**})_k((F_i^*)_2 + v_{i,k}^{w\Box}) - (C_{22}^{**})_k(F_i^*)_2]](\Gamma_{i,j}^s)_c \right. \right. \\
 &\quad \left. \left. + \left[\sum_{k=1}^{N^w-1} [(C_{12}^{**})_k((F_i^*)_2 + v_{i,k}^{w\Box}) - (C_{32}^{**})_k(F_i^*)_2]](\Gamma_{i,N-3}^s)_c \right] \right. \\
 IV_{i,j} &= \sum_{j=0}^{N-4} [(F_{i,j}^*)_1 + \sum_{k=1}^{N^w-1} [(C_{03}^{**})_k((F_i^*)_2 + v_{i,k}^{w\Box}) - (C_{23}^{**})_k(F_i^*)_2]](\Gamma_{i,j}^s)_s \\
 &\quad \left. + [(F_{i,N-3}^*)_1 + \sum_{k=1}^{N^w-1} [(C_{13}^{**})_k((F_i^*)_2 + v_{i,k}^{w\Box}) - (C_{33}^{**})_k(F_i^*)_2]](\Gamma_{i,N-3}^s)_s \right]
 \end{aligned} \tag{24}$$

Note all the symbols used in this equation are defined in Appendix C.

The right-hand side of Equation (23) can be determined depending on the motion of the hydrofoil motion of the local amplitude h_0 defined as:

$$h(\vec{x}, t) = h_0(\vec{x}) \cos \omega t \tag{25}$$

And thus the partial derivative terms in Equation (23) can be expressed as:

$$\begin{aligned}
 \frac{\partial h}{\partial t} &= \omega h_0(x) \cos \omega t \\
 \frac{\partial h}{\partial x} &= \frac{\partial h_0(x)}{\partial x} \sin \omega t
 \end{aligned} \tag{26}$$

For a simple harmonic heaving motion, $h_0(x)$ will be a constant motion amplitude, and for the pitching motion about $x = x_0$, the amplitude function and its derivative with respect to x become:

$$\begin{aligned}
 h_0(x) &= (x - x_0)\alpha_{\max} \\
 \frac{\partial h_0(x)}{\partial x} &= \alpha_{\max}
 \end{aligned} \tag{27}$$

where α_{\max} is the amplitude of the pitching motion.

Applying Equation (23) to $(N-2) \times M$ control points will result in a simultaneous equation of $2 \times (N-2) \times M$ unknowns for the cosine and sine parts of the spanwise discrete vortex strengths, that is, $(\Gamma_{i,j}^s)_c$ and $(\Gamma_{i,j}^s)_s$. The remaining terms $\Gamma_{i,N-2}^s$ and $\Gamma_{i,N-1}^s$ can be determined using the numerical Kutta condition equation.

6 Forces on hydrofoil

Quasi-steady forces on the hydrofoil are computed by summing the Kutta-Joukowski forces acting on each vortex segment $\Delta\vec{\ell}$:

$$\Delta\vec{F} = \rho\vec{V} \times \Gamma\Delta\vec{\ell} \quad (28)$$

The added mass force can be obtained by taking the derivative analytically the velocity potential expressed by the vortex strengths as shown in Appendix D.

The lift force shown in Equation (5) may then be discretized as:

$$\begin{aligned} L_1 &= -\rho \sum_{i=0}^{M-1} \sum_{j=0}^{N-1} \frac{\partial}{\partial t} \left[\sum_{k=0}^j \Gamma_{i,j}^s \right] (\Delta x_{i,j}) \\ L_2 &= -\rho U \sum_{i=0}^{M-1} \sum_{j=0}^{N-1} \Gamma_{i,j}^s \end{aligned} \quad (29)$$

We define the non-dimensional lift coefficient as:

$$C_L(t) = \frac{L(t)}{1/2\rho U^2 A \chi} \quad (30)$$

where A is the plan area of the hydrofoil and χ is the non-dimensional motion amplitude; $\chi = 2h_0/c$ for the simple heaving motion, and $\chi = \alpha_{\max}$ for the simple pitching motion. The moment coefficient about $x = x_0$ is:

$$C_M(t) = \frac{M(t)}{1/2\rho U^2 A c \chi} \quad (31)$$

The amplitude and phase of the lift coefficient are defined as:

$$\begin{aligned} C_L(t) &= a_1 \cos \omega t + b_1 \sin \omega t \\ &= \bar{C}_L \sin(\omega t - \phi_L) \end{aligned} \quad (32)$$

where

$$\bar{C}_L = \sqrt{a_1^2 + b_1^2} \quad \phi_L = \tan^{-1} \frac{-a_1}{b_1}$$

The amplitude and phase of the moment coefficient are defined similarly as:

$$C_M(t) = \bar{C}_M \sin(\omega t - \phi_M) \quad (33)$$

7 Numerical analysis

The numerical computation was performed for a hydrofoil of zero-thickness with a rectangular plan form in a simply oscillating heaving or pitching motion. The results are compared with the time-domain analysis of Lee(1977).

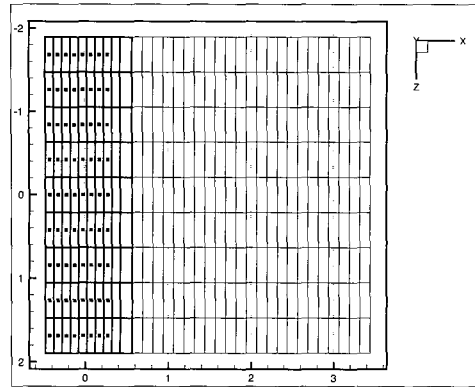


Figure 4: Vortex lattice and control point arrangements for a rectangular wing of $A.R. = 4.0$ with $N = 10$, $M = 10$ and $N^w = 24$

Figure 4 shows the vortex lattice arrangement together with the control points for a rectangular wing of the aspect ratio $A.R. = 4.0$. Note that the last two panels in the chordwise direction do not have the control points, which implies that the explicit Kutta condition is applied in this area. The number of shed wake vortices on each chordwise strip is limited to $N^w = 24$, to reduce the computing time for wake-vortex-induced velocities.

Figures 5 and 6 show the convergence test result on the number of spanwise and chordwise panels, respectively. The numbers of panels in the chordwise and spanwise directions, $N = 20$ and $M = 20$, are considered sufficient for converged solution and are used in all subsequent computations.

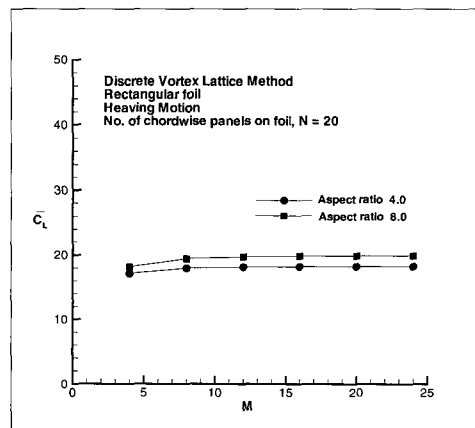


Figure 5: Effect of number of spanwise panels M on convergence

The position of the first shed vortex is chosen to be $\Delta w/4$ downstream of the trailing edge $x_{T.E.}$, if the spacings on the blade and in the wake are the same, that is $\Delta c = \Delta w$. If, however, the spacings are different from each other, the selection of the position will influence the results. The best choice for this position is known to be or at least close to $\Delta w/4$. Fortunately choice of this value is relatively less sensitive to the solution. Figure 7

The lift coefficient computed on the condition of the reduced frequency $k = \omega c/2U = \pi/2$

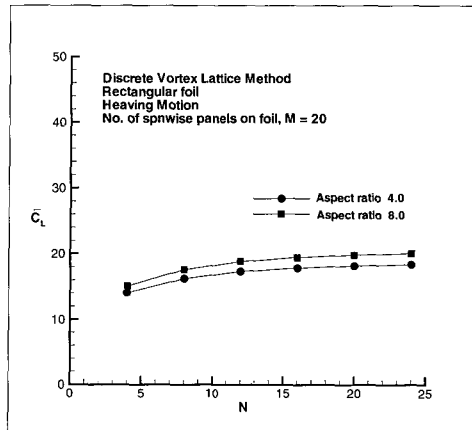


Figure 6: Effect of number of chordwise panels N on convergence

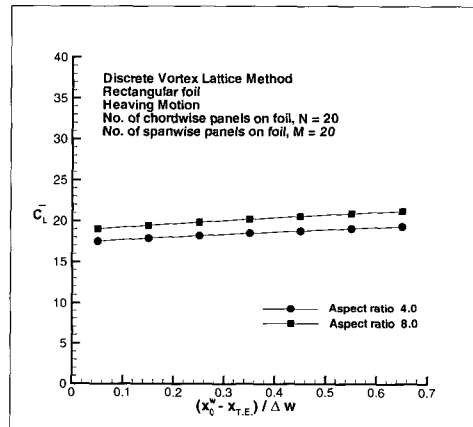


Figure 7: Effect on lift coefficient of the first shed vortex position in wake

by the present frequency-domain approach is compared with that by the time-domain approach of Lee(1977) in Figure 8. The result compares very well indicating the present formulation is valid in the unsteady force computation, except that the time-domain solution shows slightly unnatural behavior at the initial time-step. This is due to the finite-difference time derivative of the velocity potential in time-domain approach.

In Figure 9, the influence of the aspect ratio is shown less sensitive to the lift coefficient variations.

Figure 10 shows the lift coefficient variation for various reduced frequencies.

8 Conclusions

The lifting surface problem around a three-dimensional hydrofoil has been solved in the frequency domain. Existing explicit Kutta condition relation of Kerwin and Lee(1978) requires a specified functional behavior of the vorticity in space near the trailing edge in the time domain. The control in space in the frequency domain approach is formulated and implemented. Sample computations

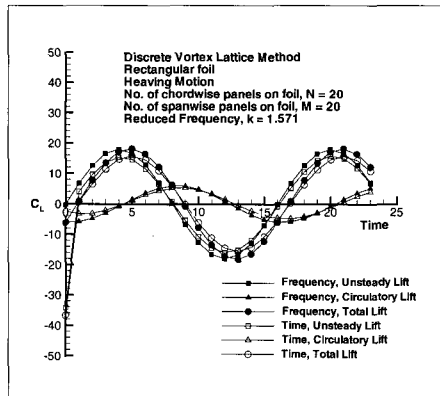


Figure 8: Comparison of lift coefficient variations obtained by frequency- and time-domain approaches for a rectangular foil of $A.R. = 4.0$

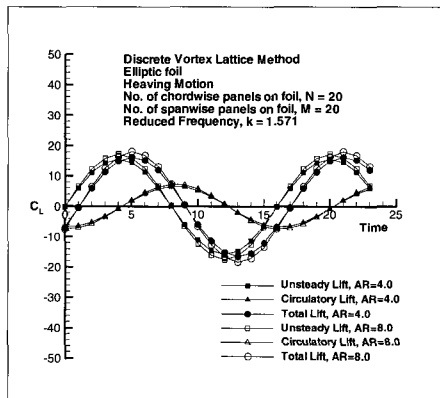


Figure 9: Comparison of lift coefficient variation for aspect ratio $A.R. = 4.0$ and $A.R. = 8.0$ of rectangular hydrofoil

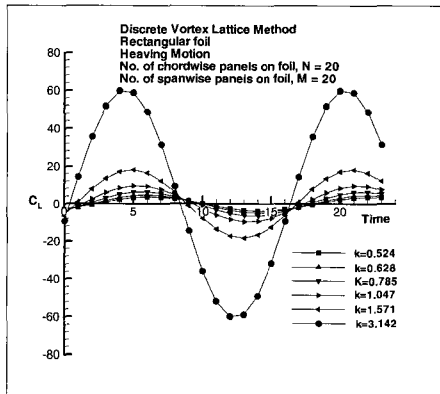


Figure 10: Comparison of lift coefficient variations for various reduced frequencies, $\pi/2 \leq k \leq \pi$

carried out according to the new formulation compares with that of Lee(1977) who solved the unsteady lifting problem in the time domain. The new formulation may now be applicable to the solution of the unsteady propeller problem with explicit Kutta condition specified.

References

- CHAI, H.B. 1990 Analysis of Unsteady 2-Dimensional Hydrofoil Problem by Discrete Vortex Method. S.M. Thesis, Department of Naval Architecture Ocean Engineering, Chungnam National University
- CHOW, C.Y. 1979 An Introduction to Computational Fluid Mechanics. Department of Aerospace Engineering Sciences University of Colorado, John Wiley and Sons, Inc.
- CUMMINGS, D.E. 1973 Numerical Prediction of Propeller Characteristics. J. of Ship Research, **17**, 1
- JAMES, R.M. 1972 On the Remarkable Accuracy of the Vortex Lattice Method. Computer Methods in Applied Mechanics and Engineering, **1**
- KERWIN, J.E. 1961 The Solution of Propeller Lifting Surface Problems by Vortex Lattice Methods. Department of Naval Architecture and Marine Engineering, M.I.T.
- KERWIN, J.E. 1973 Computer Techniques for Propeller Blade Section Design. International Shipbuilding Progress, **20**, pp. 227-251
- KERWIN, J.E. AND FRYDELUND, O. 1977 The Development of Numericals for the Computation of Unsteady Propeller Force. Symposium on Hydrodynamics of Ship and Offshore Propulsion System, Oslo, Norway
- KERWIN, J.E. AND LEE, C.S. 1978 Prediction of Steady and Unsteady Marine Propeller Performance by Numerical Lifting-Surface Theory. Trans. SNAME, **86**
- KIM, H.T. AND LEE, C.S. 1981 Solution of Unsteady Hydrofoil Problem by Discrete Vortex Method with Application to Fish Propulsion. J. of SNAK, **18**, 3
- LEE, C.S. 1977 A Numerical Method for the Solution of the unsteady Lifting Problem Rectangular and Elliptic Hydrofoils. S.M. Thesis, Department of Ocean Engineering, M.I.T.
- LEE, C.S. 1979 Prediction of Steady and Unsteady Performance of Marine Propellers with or without Cavitation by Numerical Lifting Surface Theory. Ph.D. Thesis, Department of Ocean Engineering, M.I.T., Cambridge, Mass.
- MORAN, J. 1984 An Introduction to Theoretical and Computational Aerodynamics. John Wiley and Sons, Inc.
- NEWMAN, J.N. 1977 Marine Hydrodynamics. Department of Ocean Engineering, The M.I.T. Press
- TSAO, S.K. 1975 Documentation of Programs for the Analysis of Performance and Spindle Torque of Controllable Pitch Propellers. J. of Ship Research, **17**, 1

Appendix A: 2-Point kutta condition

The explicit (2-point) Kutta condition states that the strength the last two spanwise vortices near the trailing edge be determined as a linear interpolation of the strength of the adjacent vortex as:

$$\begin{aligned}\gamma_{N-2}^s &= d\gamma_{N-3}^s + e\gamma_0^{ws} \\ \gamma_{N-1}^s &= f\gamma_{N-3}^s + g\gamma_0^{ws}\end{aligned}\quad (34)$$

where

$$\begin{aligned}e &= \frac{x_{N-2} - x_{N-3}}{x_w - x_{N-3}}, & d &= 1 - e \\ g &= \frac{x_{N-1} - x_{N-3}}{x_w - x_{N-3}}, & f &= 1 - g\end{aligned}$$

In strength of the discrete vortices, Equation (34) becomes:

$$\begin{aligned}\Gamma_{N-2}^s &= d\Gamma_{N-3}^s + e\left(\frac{\Delta f}{\Delta\omega}\right)\Gamma_0^{ws} \\ \Gamma_{N-1}^s &= f\Gamma_{N-3}^s + g\left(\frac{\Delta f}{\Delta\omega}\right)\Gamma_0^{ws}\end{aligned}\quad (35)$$

where

$$\Delta f = \frac{c}{N}, \quad \Delta\omega = U\Delta t$$

Substituting Equation (14) for the strength of the first shed vortex into (35), we will obtain (21).

Appendix B: Formation of vortex loops in trailing wake

The right-hand side of Equation (19) can be rearranged as:

$$\begin{aligned}& \sum_{i=0}^{M-1} \left\{ [-C_2 F(\vec{x}_p; i, N-2) - C_5 F(\vec{x}_p; i, N-1)] \sum_{k=1}^{N^w-1} \Gamma_{i,k}^{ws} \right\} \\ & + \sum_{i=0}^{M-1} \sum_{k=1}^{N^w-1} \left\{ v(\vec{x}_p; \vec{x}_{i,0}^{ws}) - v(\vec{x}_p; \vec{x}_{i,k}^{ws}) + \sum_{l=0}^{k-1} [v(\vec{x}_p; \vec{x}_{i+1,l}^{wc}) - v(\vec{x}_p; \vec{x}_{i,l}^{wc})] \right\} \Gamma_{i,k}^{ws} \\ & + \frac{\partial h}{\partial t} + U \frac{\partial h}{\partial x} \\ & \equiv (RHS)_1 + (RHS)_2 + \frac{\partial h}{\partial t} + U \frac{\partial h}{\partial x}\end{aligned}\quad (36)$$

At a particular time $t = \tau$, the strength of the first shed vortex in the wake may be expressed as:

$$\Gamma_0^{ws} = -\Gamma^T(t = \tau) + \Gamma^T(t = \tau - 1)\quad (37)$$

Applying the shedding mechanism, we can obtain the expression for Γ_k^{ws} as:

$$\Gamma_k^{ws} = -\Gamma^T(t = \tau - k) + \Gamma^T(t = \tau - k - 1)\quad (38)$$

The first term in the right-hand side of Equation (36) may now be rewritten as:

$$(RHS)_1 = \sum_{i=0}^{M-1} \{[-C_2 F(\vec{x}_p; i, N-2) - C_5 F(\vec{x}_p; i, N-1)] \times \sum_{k=1}^{N^w-1} [-\Gamma_i^T(\tau-k) + \Gamma_i^T(\tau-k-1)]\} \quad (39)$$

where $\Gamma_i^T(-1) \equiv 0$. The second term may be rewritten as:

$$(RHS)_2 = \sum_{i=0}^{M-1} \sum_{k=1}^{N^w-1} \{v(\vec{x}_p; \vec{x}^w) - v(\vec{x}_p; \vec{x}_k^{ws}) + \sum_{l=0}^{k-1} [v(\vec{x}_p; \vec{x}_{i+1,l}^{wc}) - v(\vec{x}_p; \vec{x}_{i,l}^{wc})]\} \times [(-\Gamma_i^T(t=\tau-k) + \Gamma_i^T(t=\tau-k-1))] \quad (40)$$

which in turn may be rearranged as:

$$(RHS)_2 = \sum_{i=0}^{M-1} \sum_{k=1}^{N^w-1} v_{i,k}^{w\Box} [-\Gamma_i^T(t=\tau-k)] \quad (41)$$

From Equations (39) and (41), it may be observed that the induced velocities due to wake vortices are represented as a function of the circulation on the blade in the pasc and the induced velocities due to the closed vortex loops.

Appendix C: Rearrangement of coefficients of time harmonics

Equation (21) may be rewritten in in time-harmonic components:

$$\begin{aligned} \Gamma_{N-2}^s &= (\Gamma_{N-2}^s)_c \cos \omega t + (\Gamma_{N-2}^s)_s \sin \omega t \\ &= d[(\Gamma_{N-3}^s)_c \cos \omega t + (\Gamma_{N-3}^s)_s \sin \omega t] \\ &\quad + e\left(\frac{\Delta f}{\Delta \omega}\right)[- \omega \Delta t [- \left(\sum_{j=0}^{N-1} \Gamma_{jc}^s\right) \sin \omega t + \left(\sum_{j=0}^{N-1} \Gamma_{js}^s\right) \cos \omega t]] \\ \Gamma_{N-1}^s &= (\Gamma_{N-1}^s)_c \cos \omega t + (\Gamma_{N-1}^s)_s \sin \omega t \\ &= f[(\Gamma_{N-3}^s)_c \cos \omega t + (\Gamma_{N-3}^s)_s \sin \omega t] \\ &\quad + g\left(\frac{\Delta f}{\Delta \omega}\right)[- \omega \Delta t [- \left(\sum_{j=0}^{N-1} \Gamma_{jc}^s\right) \sin \omega t + \left(\sum_{j=0}^{N-1} \Gamma_{js}^s\right) \cos \omega t]] \end{aligned} \quad (42)$$

To simplify the equations we introduce the following:

$$\begin{aligned} p &\equiv e\left(\frac{\Delta f}{\Delta \omega}\right)\omega \Delta t \\ q &\equiv g\left(\frac{\Delta f}{\Delta \omega}\right)\omega \Delta t \end{aligned}$$

Rearranging Equation (42) in coefficients of time-harmonics and setting the coefficient to zero, we obtain the relations:

$$\begin{aligned}
 (\Gamma_{N-2}^s)_c + p(\Gamma_{N-2}^s)_s + p(\Gamma_{N-1}^s)_s &= d(\Gamma_{N-3}^s)_c - p\left(\sum_{j=0}^{N-4} \Gamma_{js}^s\right) - p(\Gamma_{N-3}^s)_s \\
 -p(\Gamma_{N-2}^s)_c + (\Gamma_{N-2}^s)_s - p(\Gamma_{N-1}^s)_c &= d(\Gamma_{N-3}^s)_s + p\left(\sum_{j=0}^{N-4} \Gamma_{jc}^s\right) + p(\Gamma_{N-3}^s)_c \\
 (\Gamma_{N-1}^s)_c + q(\Gamma_{N-1}^s)_s + q(\Gamma_{N-2}^s)_s &= f(\Gamma_{N-3}^s)_c - q\left(\sum_{j=0}^{N-4} \Gamma_{js}^s\right) - q(\Gamma_{N-3}^s)_s \\
 -q(\Gamma_{N-1}^s)_c + (\Gamma_{N-1}^s)_s - q(\Gamma_{N-2}^s)_c &= f(\Gamma_{N-3}^s)_s + q\left(\sum_{j=0}^{N-4} \Gamma_{jc}^s\right) + q(\Gamma_{N-3}^s)_c
 \end{aligned} \tag{43}$$

Let us express the above equation in matrix form:

$$\begin{aligned}
 \vec{A} \times \vec{\Gamma} &= \vec{B} \\
 \vec{A} &= \begin{bmatrix} 1 & p & 0 & p \\ -p & 1 & -p & 0 \\ 0 & q & 1 & q \\ -q & 0 & -q & 1 \end{bmatrix}, \quad \vec{\Gamma} = \begin{bmatrix} (\Gamma_{N-2}^s)_c \\ (\Gamma_{N-2}^s)_s \\ (\Gamma_{N-1}^s)_c \\ (\Gamma_{N-1}^s)_s \end{bmatrix} \\
 \vec{B} &= \begin{bmatrix} -p\left(\sum_{j=0}^{N-4} \Gamma_{js}^s\right) + d(\Gamma_{N-3}^s)_c - p(\Gamma_{N-3}^s)_s \\ p\left(\sum_{j=0}^{N-4} \Gamma_{jc}^s\right) + p(\Gamma_{N-3}^s)_c + d(\Gamma_{N-3}^s)_s \\ -q\left(\sum_{j=0}^{N-4} \Gamma_{js}^s\right) + f(\Gamma_{N-3}^s)_c - q(\Gamma_{N-3}^s)_s \\ q\left(\sum_{j=0}^{N-4} \Gamma_{jc}^s\right) + q(\Gamma_{N-3}^s)_c + f(\Gamma_{N-3}^s)_s \end{bmatrix}
 \end{aligned} \tag{44}$$

Applying the Cramer's rule, we solve the simultaneous equation for Γ to get:

$$\begin{aligned}
 (\Gamma_{N-2}^s)_c &= \frac{1}{D} \begin{vmatrix} B_0 & p & 0 & p \\ B_1 & 1 & -p & 0 \\ B_2 & q & 1 & q \\ B_3 & 0 & -q & 1 \end{vmatrix} \\
 &= \frac{1}{D} \left[B_0 \begin{vmatrix} 1 & -p & 0 \\ q & 1 & q \\ 0 & -q & 1 \end{vmatrix} - B_1 \begin{vmatrix} p & 0 & p \\ q & 1 & q \\ 0 & -q & 1 \end{vmatrix} + B_2 \begin{vmatrix} p & 0 & p \\ 1 & -p & 0 \\ 0 & -q & 1 \end{vmatrix} - B_3 \begin{vmatrix} p & 0 & p \\ 1 & -p & 0 \\ q & 1 & q \end{vmatrix} \right]
 \end{aligned} \tag{45}$$

$$\begin{aligned}
 &= \frac{A_{00}^*}{D} B_0 - \frac{A_{10}^*}{D} B_1 + \frac{A_{20}^*}{D} B_2 - \frac{A_{30}^*}{D} B_3 \\
 &= [p(-\frac{A_{10}^*}{D}) + q(-\frac{A_{30}^*}{D})] (\sum_{j=0}^{N-4} \Gamma_{jc}^s) + [-p(\frac{A_{00}^*}{D}) - q(\frac{A_{20}^*}{D})] (\sum_{j=0}^{N-4} \Gamma_{js}^s) \\
 &\quad + [d(\frac{A_{00}^*}{D}) + p(-\frac{A_{10}^*}{D}) + f(\frac{A_{20}^*}{D}) + q(-\frac{A_{30}^*}{D})] (\Gamma_{N-3}^s)_c \\
 &\quad + [-p(\frac{A_{00}^*}{D}) + d(-\frac{A_{10}^*}{D}) - q(\frac{A_{20}^*}{D}) + f(-\frac{A_{30}^*}{D})] (\Gamma_{N-3}^s)_s
 \end{aligned}$$

where $D = \det \vec{A}$, and A_{00}^* etc are symbols introduced to simplify the derivations. We may derive the expression for other Γ 's, and rearrange as:

$$\begin{aligned}
 (\Gamma_{N-2}^s)_c &= C_{00}^* (\sum_{j=0}^{N-4} \Gamma_{jc}^s) + C_{01}^* (\sum_{j=0}^{N-4} \Gamma_{js}^s) + C_{02}^* (\Gamma_{N-3}^s)_c + C_{03}^* (\Gamma_{N-3}^s)_s \\
 (\Gamma_{N-2}^s)_s &= C_{10}^* (\sum_{j=0}^{N-4} \Gamma_{jc}^s) + C_{11}^* (\sum_{j=0}^{N-4} \Gamma_{js}^s) + C_{12}^* (\Gamma_{N-3}^s)_c + C_{13}^* (\Gamma_{N-3}^s)_s \\
 (\Gamma_{N-1}^s)_c &= C_{20}^* (\sum_{j=0}^{N-4} \Gamma_{jc}^s) + C_{21}^* (\sum_{j=0}^{N-4} \Gamma_{js}^s) + C_{22}^* (\Gamma_{N-3}^s)_c + C_{23}^* (\Gamma_{N-3}^s)_s \\
 (\Gamma_{N-1}^s)_s &= C_{30}^* (\sum_{j=0}^{N-4} \Gamma_{jc}^s) + C_{31}^* (\sum_{j=0}^{N-4} \Gamma_{js}^s) + C_{32}^* (\Gamma_{N-3}^s)_c + C_{33}^* (\Gamma_{N-3}^s)_s
 \end{aligned} \tag{46}$$

where C_{00}^* etc are symbols introduced as coefficients of $(\Gamma_j^s)_{c \text{ or } s}$ for $0 \leq j \leq N - 3$. The definition can be found by comparing (45) and (46).

The total circulation on the foil may be expressed by time harmonics as:

$$\Gamma^T(t) = \sum_{j=0}^{N-1} [(\Gamma_j^s)_c \cos \omega t + (\Gamma_j^s)_s \sin \omega t] \tag{47}$$

Using this we may derive the circulation of the past time steps as:

$$\begin{aligned}
 \Gamma^T(t = \tau - k\Delta t) &= \sum_{j=0}^{N-1} \{ [(\Gamma_j^s)_c \cos \omega k\Delta t - (\Gamma_j^s)_s \sin \omega k\Delta t] \cos \omega \tau \\
 &\quad + [(\Gamma_j^s)_c \sin \omega k\Delta t + (\Gamma_j^s)_s \cos \omega k\Delta t] \sin \omega \tau \}
 \end{aligned} \tag{48}$$

Substituting Equation (46) into Equation (48), we obtain expressions for the circulation of the past

in time harmonics of $(\Gamma_j^s)_{c \text{ or } s}$ for $0 \leq j \leq N - 3$ as follows:

$$\begin{aligned}
 & \Gamma^T(t = \tau - k\Delta t) \\
 &= \{ [(\sum_{j=0}^{N-4} \Gamma_{jc}^s)(\cos \omega k \Delta t + C_{00}^* \cos \omega k \Delta t - C_{10}^* \sin \omega k \Delta t + C_{20}^* \cos \omega k \Delta t - C_{30}^* \sin \omega k \Delta t) \\
 &+ (\sum_{j=0}^{N-4} \Gamma_{js}^s)(-\sin \omega k \Delta t + C_{01}^* \cos \omega k \Delta t - C_{11}^* \sin \omega k \Delta t + C_{21}^* \cos \omega k \Delta t - C_{31}^* \sin \omega k \Delta t)] \cos \omega \tau \\
 &+ [(\sum_{j=0}^{N-4} \Gamma_{jc}^s)(\sin \omega k \Delta t + C_{00}^* \sin \omega k \Delta t + C_{10}^* \cos \omega k \Delta t + C_{20}^* \sin \omega k \Delta t + C_{30}^* \cos \omega k \Delta t) \\
 &+ (\sum_{j=0}^{N-4} \Gamma_{js}^s)(\cos \omega k \Delta t + C_{01}^* \sin \omega k \Delta t + C_{11}^* \cos \omega k \Delta t + C_{21}^* \sin \omega k \Delta t + C_{31}^* \cos \omega k \Delta t)] \sin \omega \tau \} \\
 &+ \{ [(\Gamma_{N-3}^s)_c(\cos \omega k \Delta t + C_{02}^* \cos \omega k \Delta t - C_{12}^* \sin \omega k \Delta t + C_{22}^* \cos \omega k \Delta t - C_{32}^* \sin \omega k \Delta t) \\
 &+ (\Gamma_{N-3}^s)_s(-\sin \omega k \Delta t + C_{03}^* \cos \omega k \Delta t - C_{13}^* \sin \omega k \Delta t + C_{23}^* \cos \omega k \Delta t - C_{33}^* \sin \omega k \Delta t)] \cos \omega \tau \\
 &+ [(\Gamma_{N-3}^s)_c(\sin \omega k \Delta t + C_{02}^* \sin \omega k \Delta t + C_{12}^* \cos \omega k \Delta t + C_{22}^* \sin \omega k \Delta t + C_{32}^* \cos \omega k \Delta t) \\
 &+ (\Gamma_{N-3}^s)_s(\cos \omega k \Delta t + C_{03}^* \sin \omega k \Delta t + C_{13}^* \cos \omega k \Delta t + C_{23}^* \sin \omega k \Delta t + C_{33}^* \cos \omega k \Delta t)] \sin \omega \tau \} \\
 &\equiv [(\sum_{j=0}^{N-4} \Gamma_{jc}^s)(C_{00}^{**})_k + (\sum_{j=0}^{N-4} \Gamma_{js}^s)(C_{01}^{**})_k] \cos \omega \tau + [(\sum_{j=0}^{N-4} \Gamma_{jc}^s)(C_{02}^{**})_k + (\sum_{j=0}^{N-4} \Gamma_{js}^s)(C_{03}^{**})_k] \sin \omega \tau \\
 &+ [(\Gamma_{N-3}^s)_c(C_{10}^{**})_k + (\Gamma_{N-3}^s)_s(C_{11}^{**})_k] \cos \omega \tau + [(\Gamma_{N-3}^s)_c(C_{12}^{**})_k + [(\Gamma_{N-3}^s)_s(C_{13}^{**})_k] \sin \omega \tau
 \end{aligned} \tag{49}$$

We may derive expression for $k + 1$ by replacing k in (49) to get $\Gamma^T(t = \tau - (k + 1)\Delta t)$. Now we may rewrite (20) in time harmonics to get:

$$\begin{aligned}
 & \sum_{i=0}^{M-1} \{ [(\sum_{j=0}^{N-4} (F_{ij}^*)_1 \Gamma_{i,jc}^s) \cos \omega \tau + (\sum_{j=0}^{N-4} (F_{ij}^*)_1 \Gamma_{i,js}^s) \sin \omega \tau] \\
 &+ (F_{i,N-3}^*)_1 [(\Gamma_{i,N-3}^s)_c \cos \omega \tau + (\Gamma_{i,N-3}^s)_s \cos \omega \tau] \} \\
 &= \sum_{i=0}^{M-1} \{ (F_i^*)_2 \sum_{k=1}^{N^w-1} [-\Gamma_i^T(\tau - k\Delta t) + \Gamma_i^T(\tau - (k + 1)\Delta t)] \} \\
 &+ \sum_{i=0}^{M-1} \sum_{k=1}^{N^w-1} [v_{i,k}^{w\Box}(-\Gamma_i^T(\tau - k\Delta t))] + \frac{\partial h}{\partial t} + U \frac{\partial h}{\partial x}
 \end{aligned} \tag{50}$$

where

$$\begin{aligned}
 (F_{i,j}^*)_1 &= F(\vec{x}_p; i, j) + C_0 F(\vec{x}_p; i, N - 2) + C_3 F(\vec{x}_p; i, N - 1) \\
 (F_{i,N-3}^*)_1 &= F(\vec{x}_p; i, N - 3) + C_1 F(\vec{x}_p; i, N - 2) + C_4 F(\vec{x}_p; i, N - 1) \\
 (F_i^*)_2 &= -C_2 F(\vec{x}_p; i, N - 2) - C_5 F(\vec{x}_p; i, N - 1)
 \end{aligned}$$

Substituting Equation (49) for $t = \tau - k\Delta t$ and the similar equation for $t = \tau - (k + 1)\Delta t$ into (50), and setting the coefficients of time harmonics, we may obtain (23).

Appendix D: Force calculation

The x -component force of Kutta-Joukowski force (28) may be obtained in time harmonics as:

$$\begin{aligned}
 F_x &= \rho \sum_{m=0}^{M-1} \sum_{n=0}^{N-1} \left\{ \left[\sum_{i=0}^{M-1} \sum_{k=0}^{N+N^w-2} v_{i,k} \Gamma_{i,k} \right] + v_0 \cos \omega t \right\} \Gamma_{i,j} \delta \ell_{m,n} \\
 &= \rho \sum_{m=0}^{M-1} \sum_{n=0}^{N-1} \left\{ \left[\sum_{i=0}^{M-1} \sum_{k=0}^{N+N^w-2} v_{i,k} [\Gamma_c^{i,k} \cos \omega t + \Gamma_s^{i,k} \sin \omega t] \right] + v_0 \cos \omega t \right\} \\
 &\quad \times (\Gamma_c^{m,n} \cos \omega t + \Gamma_s^{m,n} \sin \omega t) \delta \ell_{m,n} \\
 &= \frac{\rho}{2} \sum_{m=0}^{M-1} \sum_{n=0}^{N-1} \left\{ \left[\sum_{i=0}^{M-1} \sum_{k=0}^{N+N^w-2} v_{i,k} \Gamma_c^{i,k} \right] \Gamma_c^{m,n} + \left[\sum_{i=0}^{M-1} \sum_{k=0}^{N+N^w-2} v_{i,k} \Gamma_s^{i,k} \right] \Gamma_s^{m,n} + v_0 \Gamma_c^{m,n} \right\} \delta \ell_{m,n} \\
 &+ \frac{\rho}{2} \sum_{m=0}^{M-1} \sum_{n=0}^{N-1} \left\{ \left[\sum_{i=0}^{M-1} \sum_{k=0}^{N+N^w-2} v_{i,k} \Gamma_c^{i,k} \right] \Gamma_c^{m,n} - \left[\sum_{i=0}^{M-1} \sum_{k=0}^{N+N^w-2} v_{i,k} \Gamma_s^{i,k} \right] \Gamma_s^{m,n} + v_0 \Gamma_c^{m,n} \right\} \\
 &\quad \times \cos 2\omega t \delta \ell_{m,n} \\
 &+ \frac{\rho}{2} \sum_{m=0}^{M-1} \sum_{n=0}^{N-1} \left\{ \left[\sum_{i=0}^{M-1} \sum_{k=0}^{N+N^w-2} v_{i,k} \Gamma_c^{i,k} \right] \Gamma_s^{m,n} - \left[\sum_{i=0}^{M-1} \sum_{k=1}^{N+N^w-2} v_{i,k} \Gamma_s^{i,k} \right] \Gamma_c^{m,n} + v_0 \Gamma_c^{m,n} \right\} \\
 &\quad \times \sin 2\omega t \delta \ell_{m,n}
 \end{aligned} \tag{51}$$

Note in this equation the quadratic harmonic components produce the 0-th order time-mean component.

The y -component force is similarly derived as:

$$\begin{aligned}
 F_y &= -\rho \sum_{m=0}^{M-1} \sum_{n=0}^{N-1} \left\{ \left[\sum_{i=0}^{M-1} \sum_{k=1}^{N+N^w-2} u_{i,k} \Gamma_{i,k} \right] + U \right\} \Gamma_{m,n} \delta \ell_{m,n} \\
 &= -\rho \sum_{m=0}^{M-1} \sum_{n=0}^{N-1} \left\{ \left[\sum_{i=0}^{M-1} \sum_{k=1}^{N+N^w-2} u_{i,k} (\Gamma_c^{i,k} \cos \omega t + \Gamma_s^{i,k} \sin \omega t) \right] + U \right\} \\
 &\quad \times (\Gamma_c^{m,n} \cos \omega t + \Gamma_s^{m,n} \sin \omega t) \delta \ell_{m,n} \\
 &= -\frac{\rho}{2} \sum_{m=0}^{M-1} \sum_{n=0}^{N-1} \left\{ \sum_{i=0}^{M-1} \left[\sum_{k=0}^{N+N^w-2} u_{i,k} \Gamma_c^{i,k} \right] \Gamma_c^{m,n} + \left[\sum_{i=0}^{M-1} \sum_{k=1}^{N+N^w-2} u_{i,k} \Gamma_s^{i,k} \right] \Gamma_s^{m,n} \right\} \delta \ell_{m,n} \\
 &\quad - \rho U \sum_{m=0}^{M-1} \sum_{n=0}^{N-1} \Gamma_c^{m,n} \cos \omega t \delta \ell_{m,n} - \rho U \sum_{m=0}^{M-1} \sum_{n=0}^{N-1} \Gamma_s^{m,n} \sin \omega t \delta \ell_{m,n}
 \end{aligned} \tag{52}$$

$$\begin{aligned}
 & -\frac{\rho}{2} \sum_{m=0}^{M-1} \sum_{n=0}^{N-1} \left\{ \left[\sum_{i=0}^{M-1} \sum_{k=0}^{N+N^w-2} u_{i,k} \Gamma_c^{i,k} \right] \Gamma_c^{m,n} - \left[\sum_{i=0}^{M-1} \sum_{k=0}^{N+N^w-2} u_{i,k} \Gamma_s^{i,k} \right] \Gamma_s^{m,n} \right\} \\
 & \quad \times \cos 2\omega t \delta l_{m,n} \\
 & -\frac{\rho}{2} \sum_{m=0}^{M-1} \sum_{n=0}^{N-1} \left\{ \left[\sum_{i=0}^{M-1} \sum_{k=0}^{N+N^w-2} u_{i,k} \Gamma_c^{i,k} \right] \Gamma_s^{m,n} - \left[\sum_{i=0}^{M-1} \sum_{k=0}^{N+N^w-2} u_{i,k} \Gamma_s^{i,k} \right] \Gamma_c^{m,n} \right\} \\
 & \quad \times \sin 2\omega t \delta l_{m,n}
 \end{aligned}$$

The potential jump at the n -th panel across the camber surface may be approximated $\phi_n = \sum_k^n \Gamma_k^s$, which may be used in computing the time-derivative pressure term $-\partial\phi/\partial t$. The added mass force in discretized form may now be derived as:

$$\begin{aligned}
 F_{add.} &= -\rho \sum_{m=0}^{M-1} \sum_{n=0}^{N-1} \frac{\partial}{\partial t} \left[\sum_{k=0}^n \Gamma_{m,k} \right] (\Delta A_{m,n}) \\
 &= -\rho \sum_{m=0}^{M-1} \sum_{n=0}^{N-1} \frac{\partial}{\partial t} \left[\sum_{k=0}^n [\Gamma_c^{m,k} \cos \omega t + \Gamma_s^{m,k} \sin \omega t] \right] (\Delta A_{m,n}) \tag{53} \\
 &= -\rho \sum_{m=0}^{M-1} \sum_{n=0}^{N-1} \left[\sum_{k=0}^n \Gamma_s^{m,k} \right] (\Delta A_{m,n}) \cos \omega t + \rho \sum_{m=0}^{M-1} \sum_{n=0}^{N-1} \left[\sum_{k=0}^n \Gamma_c^{m,k} \right] (\Delta A_{m,n}) \sin \omega t
 \end{aligned}$$